ELSEVIER

Journal of Nuclear Materials 241–243 (1997) 867–872

journal of nuclear materials

Divertor target profiles and recycling studies in TCV single null lower standard discharges

R.A. Pitts [a,*], Ch. Nieswand [a], H. Weisen [a], M. Anton [a], R. Behn [a], R.F. Chavan [a], M.J. Dutch [a], B.P. Duval [a], S. Franke [a], F. Hofmann [a], B. Joye [a], J.B. Lister [a], X. Llobet [a], Y. Martin [a], J.-M. Moret [a], J. Petrzilka [b], Z.A. Pietrzyk [a], V. Piffl [b], P. Reinke [c], M.E. Rensink [d], G.R. Smith [d], W. van Toledo [a]

[a] *Centre de Recherches en Physique des Plasmas, Association EURATOM–Conféderation Suisse, Ecole Polytechnique Fédérale de Lausanne, Bâtiment PPB, Ecublens, CH-1015 Lausanne, Switzerland*

[b] *Institute of Plasma Physics, Czech Academy of Sciences, Prague, Czech Republic*

[c] *Universität Basel, Institut für Physik, Klingelbergstr. 82, CH-4056 Basel, Switzerland*

[d] *Lawrence Livermore National Laboratory, University of California, Berkeley, CA 94551, USA*

Abstract

A 'standard', single null lower diverted discharge has been developed to enable continuous monitoring of the first wall conditions and to characterise the effectiveness and influence of wall conditioning in the TCV tokamak. Measurements over a period encompassing nearly 2000 ohmic discharges of varying configuration and input power show the global confinement time and main plasma impurity concentrations to be good general indicators of the first wall condition, whilst divertor target profiles demonstrate strikingly the short term beneficial effects of He glow. Good agreement, consistent with a reduction in recycling at the plates is found between the predictions of the fluid code UEDGE and the observed outer divertor profiles of T_e and n_e before and after He glow.

Keywords: TCV; Particle fuelling; Wall conditioning; Divertor plasma; Langmuir probe

1. Introduction

The creation and physics study of a wide variety of plasma equilibria is the principal aim of the variable configuration tokamak, TCV ($R = 0.88$ m, $a \leq 0.25$ m) [1]. This variability, coupled with the flexibility of the TCV control system, enhances the role of wall conditioning in preserving good plasma performance and density control since the plasma shape and position in the nearly rectangular vacuum vessel can change radically from one discharge to the next. In addition, the observed sensitivity, for example, of H-mode accessibility, density threshold and presence or absence of ELM activity to wall conditions [2], make it important to have a regularly executed reference discharge (at least once per operational day) which can be used to follow the evolution of wall pumping and discharge impurity content throughout each operational campaign. This paper describes the use of such a 'standard shot' on TCV.

2. The TCV standard discharge

In preparation for future detached divertor studies and to permit measurements with an array of tile mounted, domed single Langmuir probes built into the lower divertor target plates, the chosen reference equilibrium is a medium density ($\bar{n}_e \approx 6 \times 10^{19}$ m^{-3}), ohmic, single-null lower (SNL) discharge in deuterium. Originally at $I_p = 380$ kA ($\kappa = 1.6$, $\delta = 0.35$) and with the ∇B drift directed away from the X-pt to maintain the discharge in L-mode, I_p was later reduced to 280 kA in order to prevent

* Corresponding author. Tel.: +41-21 693 6003; fax: +41-21 693 3751; e-mail: pitts@eltcv.epfl.ch.

PII S0022-3115(96)00622-8

transition to H-mode following reversal of B_T and boronisation. Throughout this study the internal vacuum vessel surfaces were protected to $\approx 65\%$ of the total surface area by polycrystalline, isotropic graphite armour tiles covering the central column and vessel floor and roof. Gas injection for the standard shot is through a central port in the vessel floor and thus partially into the outboard divertor fan.

Fig. 1 shows the plasma equilibrium reconstruction at $I_p = 280$ kA together with the central density and gas input for two discharges either side of a toroidal field reversal, several hundred shots after a previous boronisation. On the low field side of this very 'open' configuration, the equilibrium is characterized by an extremely long poloidal depth from X-point to outboard strike point (≈ 55 cm) and a high flux expansion there (≈ 15). This leads to low ($\approx 1°$) total incidence angles at the target and connection lengths from outside midplane to target of some 30 m → 15 m in passing from the separatrix to the last point in the outboard scrape-off layer (SOL) that is connected to the inner target. Whilst a few Langmuir probes have been installed at the inside strike zone, the current polygonal geometry of the central column tiles makes interpretation difficult and data will not be discussed here.

Density feedback and preprogrammed gas injection are employed to try and attain a fixed value of $\tilde{n}_e$ before $t = 0.75$ s, at which time the gas valve is closed and the density decay is used in the standard way to extract a 'global' particle confinement time, τ_p^* where $\tau_p^* = \tau_p/(1 - R) = -N_p/\dot{N}_p$, with R the recycling coefficient and N_p the plasma electron content, obtained by FIR interferometry. Fig. 1 is a striking illustration of the increased wall pumping that can be obtained when the field line attack angles in the divertor reverse, exposing fresh tile surfaces to the plasma. It also demonstrates one of the difficulties inherent in these standard shots — presetting the correct waveforms to allow constant density to be attained before the gas cut is a matter of experience and adjustments must be made from time to time depending on the state of wall conditions.

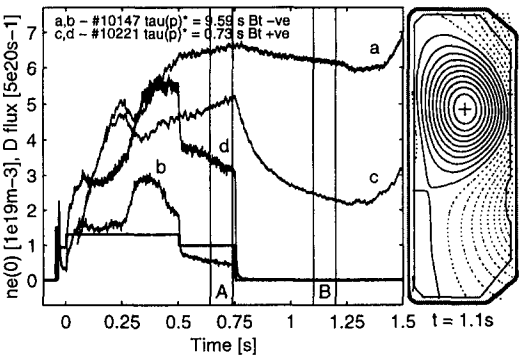

Fig. 1. Illustrating the standard shot equilibrium and demonstrating the sharp contrast in density pump-out (curves a and c) achieved by reversing the toroidal magnetic field and exposing the plasma to 'fresh' wall surfaces. The gas input (D atoms/s) is shown (curves b and d) along with the demand waveform.

3. General observations

3.1. Long term behaviour

A 'recycling' database has been constructed containing, for each standard shot, two values of the diagnostic signals comprising the database, each value obtained by averaging over the two time intervals, marked A and B in Fig. 1, just before the gas cut and near the end of the diverted phase. Fig. 2 compiles some of the data from the 146 standard shots performed during an operational period encompassing 1800 discharges of which 1026 had $I_p > 100$ kA and 350 disrupted. All standard shot numbers after 8656 have $I_p = 280$ kA and the vessel was boronised twice during this time. The latter is performed by way of a 90%He/10%B_2D_6 RF assisted glow discharge for 90 min at $T_{wall} = 200°C$. Post boronisation XPS analysis of exposed samples yields a layer thickness ≈ 100 nm with roughly depth independent B/C/O concentrations of 94/3/2 at% respectively. The relative proportions of light impurities in Fig. 2d (e.g. $p_C = n_C/(n_C + n_B + n_O)$) are computed using measurements of absolute emission from H-like ionisation stages obtained with an ultrasoft X-ray spectrometer (USX) in combination with ionisation equilibrium simulations using the IONEQ code [3]. Values of Z_{eff} in Fig. 2e are obtained using the USX impurity proportions in conjunction with soft X-ray emissivities from tomographic inversion [4].

Up to shot 9100, τ_p^* (Fig. 2c) remains low at ~ 3 s, beginning to increase thereafter and then decreasing following a second boronisation after shot 9418. Unlike the earlier phase, τ_p^* subsequently continues to increase, whilst p_B steadily decreases and p_C increases such that the sum remains constant. The remaining impurity is attributed largely to oxygen whose concentration has remained low in TCV following the first vessel boronisation. The onset of this increase in τ_p^* and decrease in boron content correlates well with the start of a protracted experimental programme (first discharge 9588) designed to investigate the dependence of energy confinement on plasma shape and comprising some 290 discharges limited on the central column tiles. It thus appears plausible that the increased wetted surface leads to more effective erosion of the deposited boron layer and in turn to degradation of the overall wall pumping capacity.

Also of note is the increase in $\tilde{n}_e$ occurring after shot 9100 due to slight changes in the programmed waveforms to permit the attainment of more reproducible densities at the gas cut. This correlates both with an increase in τ_p^* and Z_{eff} and a decrease by up to a factor of 3 in the D_α

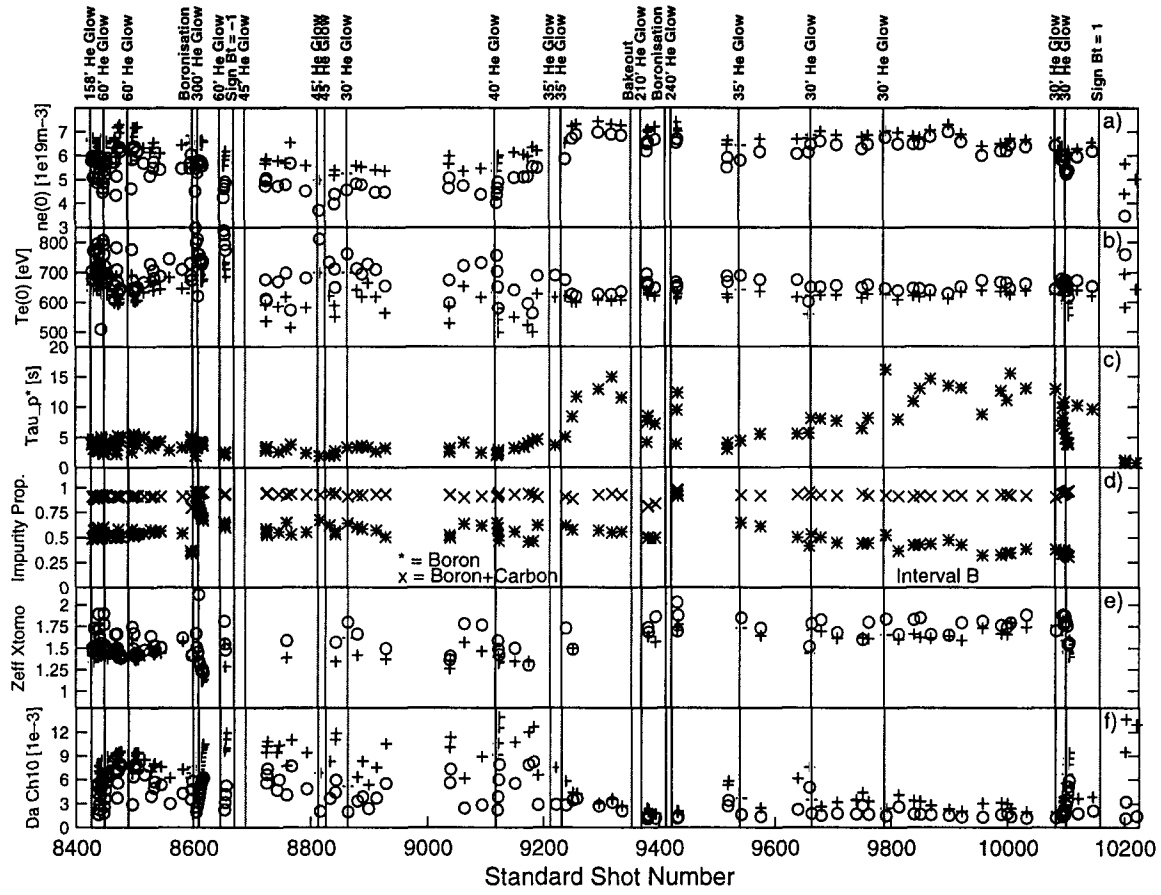

Fig. 2. Long term development of the standard shot series up to the last discharge before the 1996 summer vessel opening. He glow periods ≥ 30 min and vessel boronisations are marked by the vertical lines. In all cases except the impurity proportions (curve d) and confinement times (curve c), points for time intervals A and B are shown (the global confinement time can only be computed once during the discharge after the gas cut). The change from $I_p = 380$ kA to $I_p = 280$ kA occurs after shot 8656. Interval A (+), interval B (○).

light intensity along 10 available viewing chords covering the entire plasma cross-section (Fig. 2f shows one such chord viewing the region above the outside strike zone). The effect may be interpreted as due to a rather strong increase of particle confinement with density (the measured τ_E (electrons only) increases by $\approx 25\%$). This is supported both by the observed increase in τ_p^* and by calculations of Z_{eff} using USX impurity concentrations deduced from IONEQ which, in addition to profiles of n_e and T_e, require that a value of $D_\perp$ for the impurities be specified. If the same value of $D_\perp$ is used at both densities, the resultant Z_{eff} tends to decrease at the higher densities whilst that computed from soft X-ray emissivity (see Fig. 2e) and Bremsstrahlung measurements increases. The discrepancy can be reduced if a lower impurity diffusion coefficient (and hence longer impurity confinement time) is chosen in IONEQ simulations at the higher density. More specific experiments using the standard shot are planned to study the effect of plasma density on particle transport.

3.2. Response to He glow and boronisation

In Fig. 3, the early period of Fig. 2 at $I_p = 380$ kA is replotted for time interval B including data for n_e, T_e and V_f from a Langmuir probe ≈ 4 cm from the separatrix at the outside strike point (Fig. 3b, d and e). The impurity proportions in Fig. 3g contrast clearly the abrupt shift from a roughly equal share between B and C before boronisation at shot 8600, to almost complete replacement of C by B. (Note that p_B consistently exceeds p_C but that this is reversed just before boronisation. This is a consequence of a series of deliberately provoked vertical disruptions which succeeded in redistributing boron and carbon with a consequent increase in the plasma oxygen concentration.) Several operation days later, standard shots show the C/B ratio once again to approach unity, but good wall pumping is retained and discharge performance in other configurations is not compromised. This, together with the clear increase in τ_p^* seen in Fig. 2 when large (compared to diverted equilibria) surface areas are wetted by the plasma

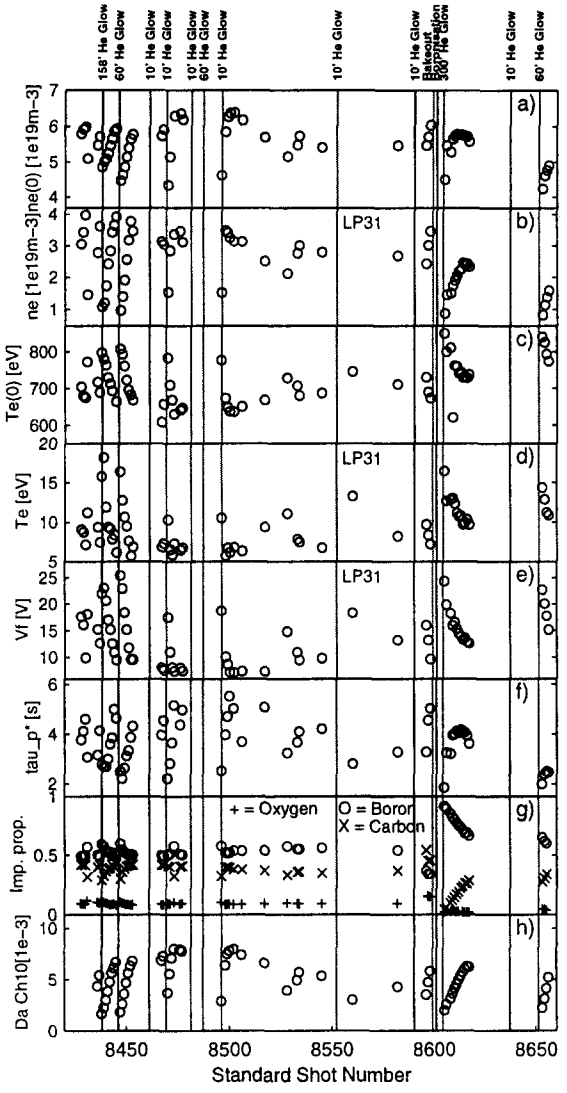

Fig. 3. Expanded region of standard shot series at $I_p = 380$ kA demonstrating the effect of varying He glow periods and boronisation. For clarity, only data for interval B (after the gas cut) are plotted; b, d and e are signals from Langmuir probe 31, the nearest of the floor probes to the outboard strike point.

during limiter discharges, indicates that wall surfaces other than those in contact with the directed SOL particle flux (for example the strike zones in the diverted standard shot) are also important in controlling recycling.

During the shot period 8437 → 8550, some 900 discharges after the previous boronisation, He glow periods of 158, 60 and 10 min were compared using the standard discharge. The variations in $\tilde{n}_e$ seen in Fig. 3a are due simply to insufficient gas injection following glow to account for the increased wall pumping. Clearly, 60 min of glow are more effective than 10 min in maintaining lower recycling, but on the basis of this limited study, there would appear to be little difference between 60 and 158 min. In all cases, the short term benefits (i.e. the first discharge after the glow period), are similar.

As shown by the probe signals n_e, T_e and V_f in Fig. 3b, d and e and the profiles in Fig. 4, the effect of Helium glow is very marked in the scrape-off layer. In Fig. 4 measured profiles are plotted at the outboard divertor strike zone for two standard shots either side of a 158 min period of He glow. In each case, the data have been both smoothed in time and linearly interpolated in radius amongst the 10 probes available in order to remove some of the larger fluctuations, especially in T_e, deeper into the SOL. The data are plotted as a function of the probe distance from the separatrix as computed from the magnetic equilibrium reconstruction derived from in-vessel poloidal magnetic field measurements. At later times in the discharge, the probe/separatrix distance for each probe has increased, corresponding to a drift in time of the strike point towards smaller radii. This movement is also clearly seen on video images of the plasma cross-section and is due to adjustments in the equilibrium as the ohmic field crosses zero.

Near the separatrix (the probe closest to the nominal strike point was unfortunately lost before the standard shot was established), the conditioning reduces the density by a factor of 3 and increases T_e by up to a factor of 2. The overall effect on the T_e profile is less marked, whilst that of the density appears to flatten considerably, indicating an increase in the SOL width. This behaviour is reproducible from one glow period to the next and is due predominantly to a decrease in the recycling coefficient (although since $\tilde{n}_e$ also decreases considerably between these two discharges, an additional effect due to changes in particle confinement cannot be isolated without more detailed measurements). The decrease in recycling is also clearly seen as a decrease in the D_α light intensity following glow — Fig. 3h illustrates this for a diode viewing the outside strike zone, but the decrease is observed everywhere on the plasma cross-section.

Prior to He glow (shot 8437), n_e near the separatrix is considerably higher than further upstream, where Thomson scattering yields $\tilde{n}_e \approx 1.8 \times 10^{19}$ m^{-3} at the 95% flux surface for this discharge (measurements in upstream SOL are not yet available on TCV). Following He glow, the large reduction in divertor density is accompanied by a decrease of only around 10% in the 'upstream' value ($n_e \approx 1.6 \times 10^{19}$ m^{-3} at 95% of the poloidal flux). Thus, although scalings have not yet been established, these results imply a transition in the outboard divertor from a 'high recycling' regime in which a scaling of the form $n_{e(div)} \propto n^3_{e(midpl)}$ would be expected [5], to a sheath limited, or linear regime, in which $n_{e(div)} \propto n_{e(midpl)}$.

The floating potential, everywhere positive in the outer divertor fan, increases by a factor of 2 across the entire profile in these shots with positive B_T (negative field reverses the polarity of V_f). Since the observation of

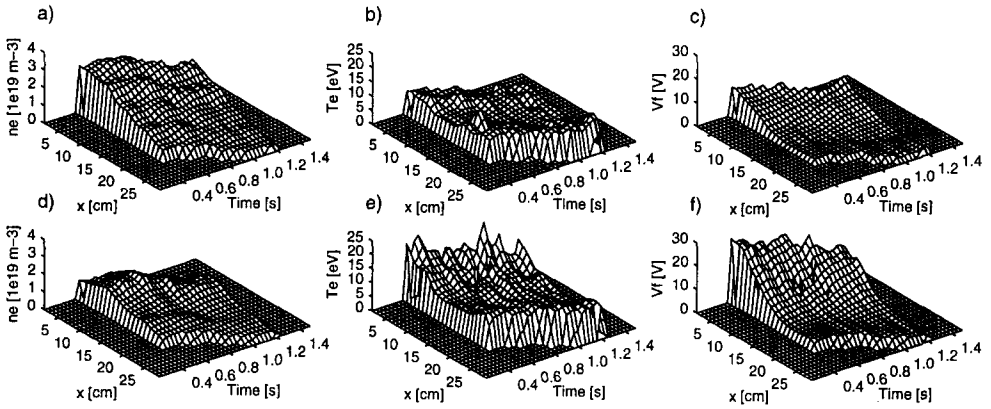

Fig. 4. Outboard divertor profiles of n_e, T_e and V_f before and after 160 min of He glow (profiles a–c shot 8437, profiles d–f shot 8438). The quantity x is the distance from the strike point.

non-zero floating potential already indicates net current flow between inboard and outboard divertor strike zones and hence asymmetries in the divertor electron temperatures [6], the increase in V_f is indicative of an exacerbation of this asymmetry following He glow.

4. Comparisons with UEDGE

As a first step towards future applications with respect to the more complex question of divertor detachment (partial detachment, at least at the outboard divertor strike point, has already been observed in a high density variant of this standard equilibrium), an attempt has been made to apply the edge fluid code UEDGE [7] to the divertor profile data in Fig. 4. In this case, one might hope to reproduce the effects of a reduction in plate recycling of ions into neutrals as a consequence of He glow. For each of the discharges 8437 and 8438, UEDGE simulations have been performed for $t = 0.8$ s, 50 ms after the gas cut. The results are compared with Langmuir probe data in Fig. 5, where each experimental point represents an average of data obtained during the interval $0.79\ \text{s} \leq t \leq 0.81$ s and the error bars the associated standard deviation. The probe density values are also associated with additional errors due to the usual uncertainties in the projected surface area.

To produce the simulated profiles, a grid of 22 (radial) $\times$ 34 (poloidal) cells is employed, with closer radial spacing near the separatrix and extending outward 1.3 cm beyond the separatrix at the midplane (beyond this point a second X-point at the top of the vessel breaks connectivity to the inside strike zone) and inwards to the 98% flux surface. A single neutral species is assumed to diffuse in the divertor fan by charge–exchange and elastic scattering. There are no impurities or drifts in the model and no particle sources other than the main plasma and recycling at the divertor plates. Values of n_e and T_e at the 98% surface are determined by interpolation of the closest available Thomson scattering points.

Simulations are run for varying R and $D_\perp$ and with fixed $\chi_{\perp e,i} = 0.5\ \text{m}^2\ \text{s}^{-1}$ for both discharges — the results are much less sensitive to changes in the latter compared with modifications to the recycling and anomalous perpendicular diffusion coefficients. Good agreement for shot 8437 is obtained for $R = 0.95$, $D_\perp = 0.5\ \text{m}^2\ \text{s}^{-1}$, whilst the combination, $R = 0.89$, $D_\perp = 0.8\ \text{m}^2\ \text{s}^{-1}$ provides a reasonable fit to the data of shot 8438. Although the simulated profiles are in general more sensitive to variations in R than in $D_\perp$, increases in the latter are efficient in reproducing the rather broad experimental profile. In both cases, the shape and even the absolute values of the measured density near the separatrix are encouragingly well reproduced by UEDGE. The long connection lengths lead to a density and temperature peaking somewhat outside the separatrix, but there are insufficient points on the experimental profile to verify this. Assuming a constant particle confinement time for these two discharges, the decrease in R would lead to a factor of 2.2 increase in τ_p^*. This should be compared with the measured values (see Fig. 3f) of 4.2 s (#8437) and 2.8 s (#8438), a decrease of 1.5 and clearly in qualitative agreement.

Conditions in this high flux expansion outboard divertor represent a rather sensitive regime for the code and convergence to a solution is slow. At values of R very near unity (e.g. $R = 0.98$), the divertor plasma is in a state of thermal collapse ($T_e = 1$–2 eV) with the ionization front being located at some distance in between the X-point and the plate. As R decreases, temperatures near the target increase and the front reattaches to the plate — analysis of the ionisation contours shows the case $R = 0.95$ to be on the boundary at which detachment occurs. This standard

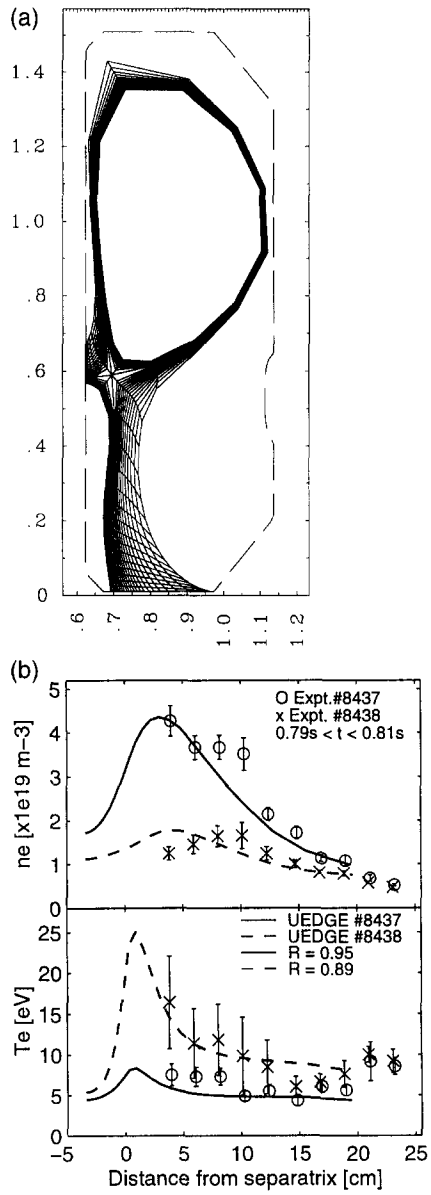

Fig. 5. UEDGE computational mesh for TCV standard shot 8437 at $t = 0.8$ s and comparison of Langmuir probe n_e and T_e profiles with UEDGE simulations assuming a different recycling coefficient before and after He glow.

discharge thus offers exciting possibilities for the study of divertor detachment and will be the focus of forthcoming experiments of this nature on TCV.

5. Conclusions

A diverted, SNL standard discharge, which is now performed at the start of every operational day, has been established on TCV and used to study the long term evolution of wall conditions. Clear correlations are observed between global particle confinement times (τ_p^*) and light impurity discharge content. The latter is also strongly dependent on the type of equilibrium (limiter/divertor) being run at any particular time during machine operation. Helium glow discharge conditioning has a strong effect on electron temperatures and densities measured at the outboard divertor strike zone, consistent with an expected reduction in recycling at the divertor targets. This is demonstrated by the good agreement that is found between experimentally measured divertor profiles before and after glow discharge and UEDGE code simulations using the recycling coefficient as the main adjustable parameter.

Acknowledgements

The authors wish to thank the TCV team for excellent support in making these measurements possible and Holger Stupp for XPS analysis of the samples exposed during boronisation. This work was partly supported by the Fonds National Suisse de la Recherche Scientifique. The installation of and support in running UEDGE at CRPP was performed by MER and GRS under US Department of Energy contract No. W-7405-Eng-48.

References

[1] F. Hofmann et al., Plasma Phys. Controlled Fusion 36 (1994) B277.
[2] H. Weisen et al., Plasma Phys. Controlled Fusion 38 (1996) 1137.
[3] H. Weisen, V. Piffl et al., 22nd Eur. Conf. on Controlled Fusion and Plasma Physics, Bournemouth, Vol. 2 (1995) p. 393.
[4] H. Weisen, D. Pasini, A. Weller and A.W. Edwards, Rev. Sci. Instrum. 62 (1991) 1531.
[5] C.S. Pitcher and P.C. Stangeby, Plasma Phys. Controlled Fusion, submitted.
[6] A.V. Chankin, these Proceedings, p. 199.
[7] T.D. Rognlien, J.L. Milovich, M.E. Rensink and G.D. Porter, J. Nucl. Mater. 196–198 (1992) 347.